

LEPTON SCATTERING AND QCD*

BY D. H. PERKINS

Nuclear Physics Department, Oxford University, Oxford, England

(Received July 25, 1979)

A comparison is made between QCD predictions and the moments of the structure and fragmentation functions measured in lepton-nucleon scattering. The data are quantitatively consistent with the leading order theory, for $q^2 > 1 \text{ GeV}^2$. The fits are not so good when present calculations of next to leading order corrections are taken into account. Moments of the structure and fragmentation functions of the gluons are in rough accord with expectations.

Introduction

This report is not meant to be a comprehensive review of lepton-nucleon scattering vis-a-vis QCD. I have concentrated on those topics with which I was familiar because I had been working on them. Many of the experimental results, particularly on quark/gluon fragmentation, are unpublished and very preliminary, and cannot be regarded as definitive. They merely illustrate some of the interesting work — and problems — which lie ahead in this field.

Comparisons of data from lepton-nucleon (eN, μ N, ν N) scattering with QCD predictions fall under several headings. In decreasing order of experimental/theoretical credibility these main topics are:

(i) *Structure Function Moments.* The most definite, unambiguous and quantitative predictions of QCD are for the moments of the structure functions F_2 and xF_3 in inclusive lepton-nucleon scattering. These moments have been evaluated in several experiments and, at least in the q^2 range 1–100 GeV^2 , the data is in fair agreement with the leading order theory. There are still problems with $2xF_1$ or $R = \sigma_S/\sigma_T$, which is hard to measure; with higher-order corrections, which seem to fit the data less well; and between experiments, where there are serious discrepancies.

(ii) *Fragmentation Function Moments.* So far, only preliminary data is available, all from bubble chamber neutrino experiments. There are experimental problems, for example from uncertainty on how to define those hadrons which are “current fragments”. The

* Presented at the XIX Cracow School of Theoretical Physics, Zakopane, June 3–17, 1979.

theory is also on less solid ground — there are questions about factorization — but even so, quantitative agreement with leading order QCD predictions is again apparent.

(iii) *Transverse Hadron Distributions*. Perturbative QCD predictions are available for several hadronic quantities, for example the sphericity, thrust, mean p_T of hadrons and the angular distribution of energy flow in the current jet, all as a function of q^2 . Unfortunately, at the values of q^2 so far available, it is clear that non-perturbative (and uncalculable) effects dominate the situation, and despite a formidable amount of experimental analysis, no real quantitative conclusions can be drawn.

(iv) *Multi-jet Events*. Clearly one of the most convincing demonstrations of the quark + gluon model would be to detect separate hadron jets, with appropriate quantum numbers, from fragmentation of quarks and gluons. There is no evidence at all for such effects in any data I know of, and it seems likely that, as under (iii), the q^2 range available in present experiments is insufficient.

In what follows, I shall discuss only structure and fragmentation function moments and ignore (iii) and (iv) completely. Some of these topics will be discussed by Sachrajda in his lecture. In this write-up, I have included a couple of graphs, one of a log moment plot from the CDHS collaboration, the other of (π^-/π^+) fragmentation ratios, which I did not include in the lecture.

PART I

Structure Function Moments

Details of the measurement and evaluation of the structure functions F_2 , xF_3 in electron, muon and neutrino scattering can be found in the original papers to which reference is made below. All the measurements of moments have involved combinations of data from different experiments. The ABCLOS bubble chamber group [1] combined low energy-data from v/\bar{v} interactions in Gargamelle at the PS with high energy data from v/\bar{v} interactions in BEBC at the SPS. The E98 collaboration [2–4] combined their own data on μp and μd scattering at FNAL with that of low energy ep and ed experiments by the SLAC–MIT group [5]. Finally, the CDHS counter group have combined their v/\bar{v} SPS data [6] (measuring F_2^{vN} and xF_3^{vN}) with SLAC ed data (measuring F_2^{eN}) using the quark model for relative normalization.

1.1. Non-Singlet Moments (xF_3 , $F_2^{\mu p} - F_2^{\mu n}$)

In leading order the strong coupling constant between quarks and gluons has the form

$$\alpha_s(q^2)/\pi = \frac{12}{(33-2m)(\ln q^2/\Lambda^2)}, \quad (1)$$

where m is the number of quark flavours, Λ is an arbitrary scale constant and $\ln q^2/\Lambda^2 \gg 1$. The moments of the structure functions have the general form

$$M(q^2) = \sum_{i=1}^3 A_i/(\ln q^2/\Lambda^2)^{d_i}, \quad (2)$$

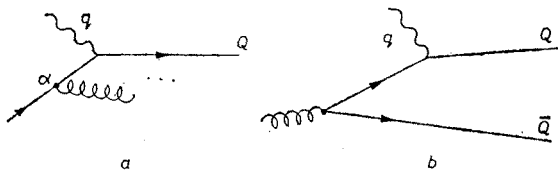
where the A_i are arbitrary coefficients but the anomalous dimensions d_i are provided by the theory. The three terms in (2) correspond to the contributions from the (flavour non-singlet) valence quarks, and those from the (singlet) quark-antiquark sea and gluons. For the valence quarks there is just the one term

$$M_3(N, q^2) = \text{const}/(\ln q^2/\Lambda^2)^{d_{\text{NS}}}, \quad (3)$$

where

$$d_{\text{NS}} = \frac{4}{(33-2m)} \left[1 - \frac{2}{N(N+1)} + 4 \sum_{j=2}^N \frac{1}{j} \right]. \quad (4)$$

The only radiative correction to the non-singlet corresponds to diagram (a); other terms such as the $G \rightarrow Q\bar{Q}$ in (b) are not involved. The anomalous dimension d_{NS} corresponds to the probability in (a) of finding a quark



in a quark [7]; the square bracket in (4) comes from the Williams-Weizsacker formula for a fermion to radiate a massless vector boson (gluon).

Comparison of the prediction (3) is made with the Nachtmann moments of xF_3 , i.e. instead of

$$M_3(N, q^2) = \int_0^1 x^{N-2} \cdot xF_3(x, q^2) dx \quad (5)$$

one uses [9]

$$M_3(N, q^2) = \int_0^1 \frac{\xi^{N+1}}{x^3} xF_3(x, q^2) \left[\frac{1 + (N+1) \sqrt{1 + 4M^2 x^2/q^2}}{N+2} \right] dx, \quad (6)$$

where

$$\xi = \frac{2x}{1 + \sqrt{1 + 4M^2 x^2/q^2}} \quad (7)$$

is the Nachtmann [8] variable. The use of ξ instead of x takes account of a kinematic correction M^2/q^2 depending on the target (nucleon) mass.

Figs 1 and 2 show the results for the Nachtmann moments of the non-singlet xF_3^{vN} from the ABCLOS collaboration [1] and for the non-singlet $(F_2^{\mu\text{p}} - F_2^{\mu\text{n}})$ from the E98 experiment [4].

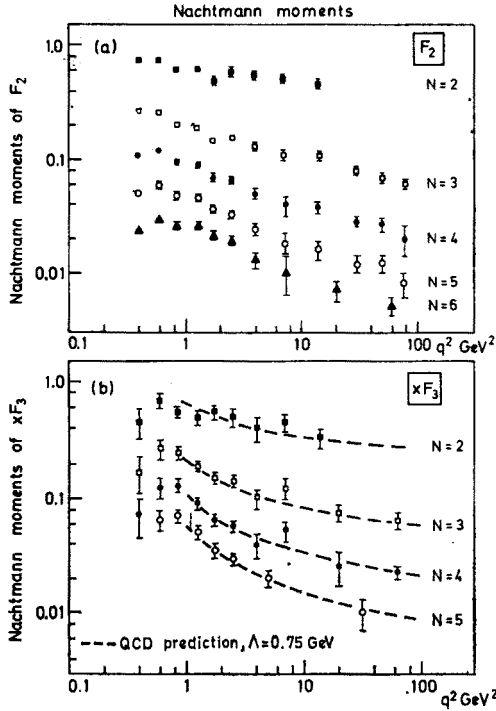


Fig. 1. Nachtmann moments of the structure functions F_2^{vN} and xF_3^{vN} , as measured by Bosetti et al. [1] (ABCLOS collaboration)

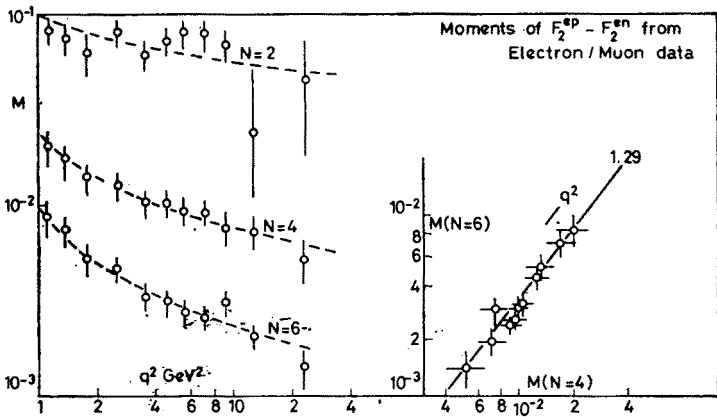


Fig. 2. Nachtmann moments of the non-singlet function $(F_2^{ep} - F_2^{en})$ from electron and muon scattering data on hydrogen and deuterium (E98 collaboration, Quirk [4]). On the right is a log-log moment plot, with line indicating QCD prediction for the slope

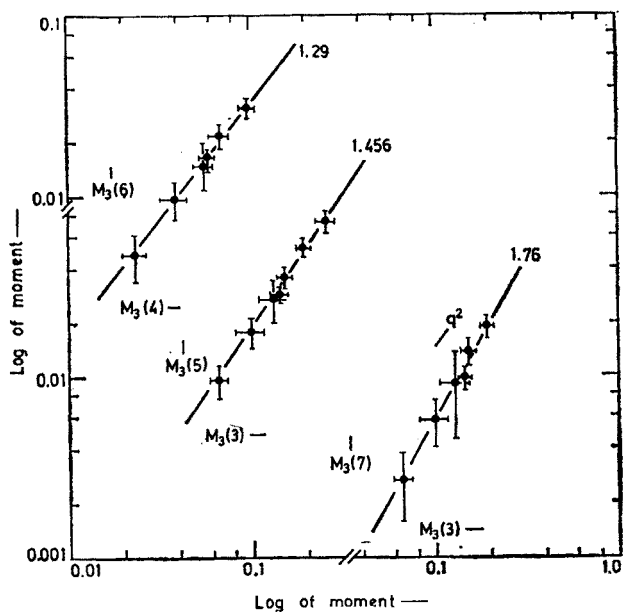


Fig. 3. Log-log plot of various non-singlet moments, ABCLOS data (Bosetti et al. [1]). Lines indicate QCD predicted slopes

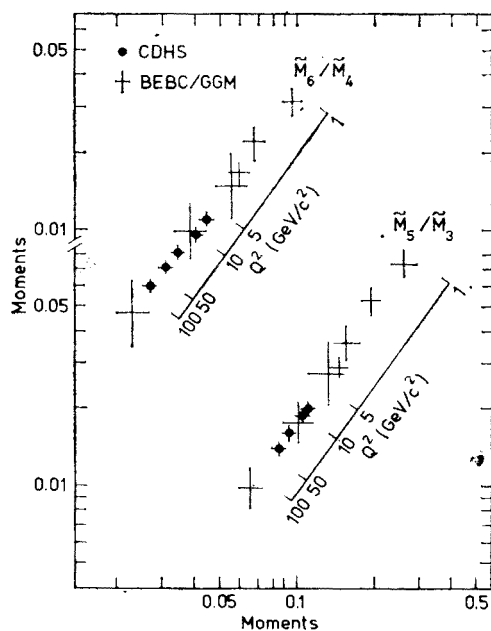


Fig. 4. Log-log plot of non-singlet moments, CDHS data (de Groot et al. [6]). (a) Cornwall-Norton moments, (b) Nachtmann moments

The first test of the leading order (LO) QCD formula (3) is that the moments of different N will be related by power laws

$$M_3(N', q^2) = K \cdot [M_3(N, q^2)]^{d'_{NS}/d_{NS}}, \tag{8}$$

where the index is the ratio of anomalous dimensions in the two cases, with the colour-flavour factor $4/(33-2m)$ cancelling. Figs 2, 3 and 4 show the log moment plots from the muon and neutrino experiments. Clearly, they are all consistent with the slopes expected from QCD. Some actual numbers are shown in Table I. In the final column, the slope for scalar gluons is given. While the ABCLOS results are close to the QCD prediction, the CDHS data fall half way between vector and scalar predictions.

TABLE I
Anomalous dimension ratios (Nachtmann Moments)

| Moments | QCD Prediction | Observed Slopes | | Scalar Gluon |
|-----------------|----------------|--|---|--------------|
| | | ABCLOS ($\nu, \bar{\nu}$) $q^2 = 1-100$ | CDHS ($\nu, \bar{\nu}$) $q^2 = 6.5-75$ | |
| $N' = 6, N = 4$ | 1.29 | 1.29 ± 0.06 | 1.18 ± 0.09 | (1.06) |
| $N' = 5, N = 3$ | 1.456 | 1.50 ± 0.08 | 1.34 ± 0.12 | (1.12) |
| $N' = 7, N = 3$ | 1.760 | 1.84 ± 0.20 | — | (1.16) |
| $N' = 6, N = 3$ | 1.621 | — | 1.38 ± 0.15 | (1.14) |

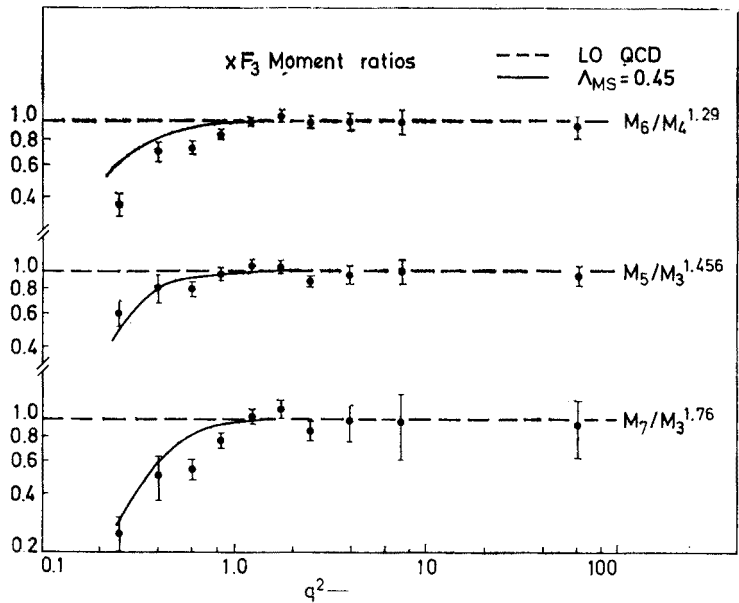


Fig. 5. Plots from Bosetti et al. [1], showing ratios $M_i^{(d_j/d_i)}/M_j$ of non-singlet moments against q^2 , which are predicted to be constant by QCD in leading order. For $q^2 < 1$, all ratios decrease. The curves take into account next to leading order corrections

Although the log moment plot has become a popular way of displaying the data, it is not the best way to present the result. Fig. 5 shows a plot of the ratio of the two sides in equation (8), which should be a constant independent of q^2 . The BEBC/GGM ratios are indeed constant for $q^2 > 1$, but show substantial deviations at lower q^2 . The solid curves show the effect of second-order corrections, discussed later. Although these show the same trend as the data, this is not support for the correction terms; individual moments fail to fit the data for $q^2 < 1$, just as badly as the leading order formula.

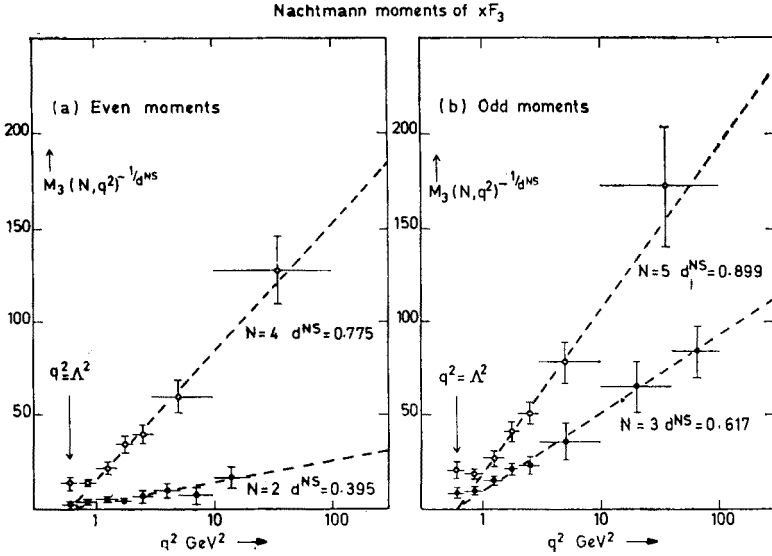


Fig. 6. Plot of $M^{-1/d}$ versus $\ln q^2$. QCD predicts a straight line relation. ABCLOS data

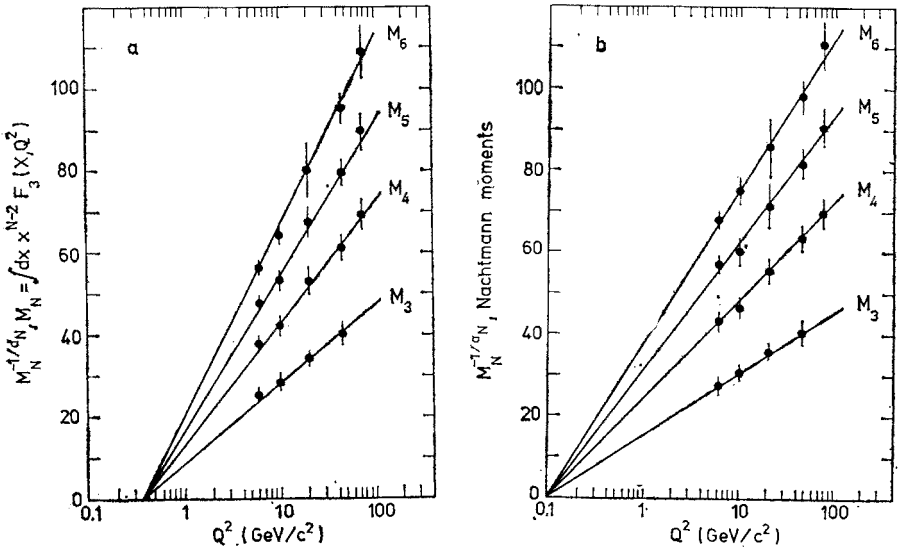


Fig. 7. Plots as in Fig. 6, for CDHS data

The second test of equation (3) is to demonstrate the $\ln q^2$ dependence of the moments, via the equation

$$[M_3(N, q^2)]^{-1/d_{NS}} = \text{const} (\ln q^2 - \ln \Lambda^2). \tag{9}$$

Figs 6 and 7 show that the quantity in (9) on the LHS is indeed linear with $\ln q^2$ for $q^2 > 1$. This linearity is a vital test of QCD, since only an asymptotically free gauge theory contains such logarithmic dependence.

Examination of Figs 6 and 7 shows that there are severe discrepancies in the values of the moments at the same q^2 in the different experiments. The quantity $M^{-1/d_{NS}}$ is about a factor 2 larger in the bubble chamber than in the counter neutrino experiment, for all N values, and they differ greatly in the value of the extrapolation point, $\ln \Lambda^2$. Table II

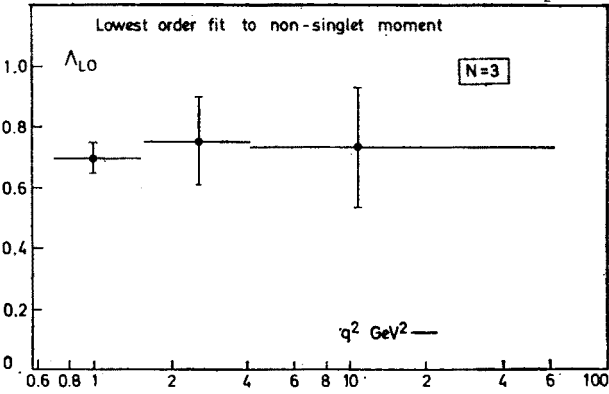


Fig. 8. Scale parameter Λ_{LO} calculated from leading order QCD fits to $N = 3$ non-singlet moment, in different ranges of q^2 (ABCLOS data)

TABLE II

| Λ_{LO} values ($m = 3$)* | | | | | | |
|------------------------------------|-----------------|-----------------|-----------------|-----------------|-----------------|----------------------|
| Experiment | $N = 3$ | $N = 4$ | $N = 5$ | $N = 6$ | $N = 7$ | Global (All N) |
| ν ABCLOS [1] $q^2 > 1$ | 0.70 ± 0.08 | 0.76 ± 0.07 | 0.77 ± 0.07 | 0.78 ± 0.08 | 0.75 ± 0.07 | 0.75 ± 0.05 |
| μ E98 [4] $q^2 > 1$ | — | 0.73 ± 0.09 | — | 0.77 ± 0.07 | — | 0.73 ± 0.10 |
| ($R = 0.2$) [3] $q^2 > 3$ | — | — | — | — | — | 0.70 ± 0.07 |
| ν CDHS [6] $q^2 > 6.5$ | 0.41 ± 0.13 | 0.42 ± 0.12 | 0.38 ± 0.10 | 0.33 ± 0.10 | — | 0.39 ± 0.08 |

* The value of Λ depends weakly on m : $d\Lambda/dm = -0.05 \text{ GeV}$.

shows results from the two neutrino experiments as well as that from muon scattering. An obvious difference is that in the CDHS experiment, the minimum q^2 is large. However, as shown in Fig. 8, there is no substantial dependence of A on q^2 in the ABCLOS data.

One point of difference is that the first two experiments in Table II included elastic events ($x = 1$) in evaluating moments. While it is true that for $q^2 > 6$ elastic events have little effect for $N = 3$, this is not true for high N (see below).

A final point is that the CDHS and E98 analyses have used F_2 values from ep, ed experiments, and these involve uncertainties in R , such that $dA/dR \approx -1$ GeV. The ABCLOS data is unique in depending on $xF_3^{\nu N}$ only, a quantity which is independent of assumptions about R [1]. I do not think however that any of these factors is going to bring the CDHS result into agreement with the ABCLOS/E98 values. It is perhaps fair to point out that, not using moments but only the $\nu, \bar{\nu}$ data covering part of the q^2 range at each x value, to parametrize the parton distributions in the form $x^\alpha(1-x)^\beta$, the CDHS group [6] come out with bigger A values (~ 0.55 GeV).

1.2. Singlet moments

In QCD, the moments of $F_2(x, q^2)$, measuring the momentum of quarks plus antiquarks, consists of three terms, as in (2). Thus one can write

$$M_2(N, q^2) = M_{NS}(N, q_0^2) (L_0/L)^{d_{NS}} + M_+(N, q_0^2) (L_0/L)^{d_+} + M_-(N, q_0^2) (L_0/L)^{d_-}, \quad (10)$$

where the last 2 terms are the singlets, $L = \ln q^2/\Lambda^2$, $L_0 = \ln q_0^2/\Lambda^2$, and d_{NS} , d_+ and d_- are anomalous dimensions given in the Appendix. For neutrino scattering from an isoscalar target, with θ (Cabibbo) $\simeq 0$, so that s, \bar{s} contributions are neglected, the coefficients M_{NS} , M_+ and M_- , for $m = 3$, can be simply expressed in terms of the moment $M_2(N, q_0^2)$ of quarks + antiquarks at q_0^2 , and that, $M_G(N, q_0^2)$ of the gluons:

$$M_{NS}(q_0^2) = \frac{1}{3} M_2(N, q_0^2),$$

$$M_+(q_0^2) = \frac{2}{3} [(1 - A_N)M_2(N, q_0^2) + B_N M_G(N, q_0^2)],$$

$$M_-(q_0^2) = \frac{2}{3} [A_N M_2(N, q_0^2) - B_N M_G(N, q_0^2)], \quad (11)$$

where the coefficients A_N , B_N are also given in the Appendix (see also Ref. [13]). The exact formula is more complicated, but the neglected terms in s, \bar{s} are extremely small ($\approx 10^{-3}$ if we base our estimates of the s, \bar{s} sea from antineutrino dimuon data and the GIM charm model). Equations (10) and (11) allow $M_G(N, q_0^2)$ to be deduced from $M_2(N, q^2)$, if A , and hence L_0/L , is known.

The main point is that $M_2(N, q^2)$ decreases as q^2 increases on account of the radiative correction to the non-singlet (the first term in (10)), but it falls less rapidly than $M_3(N, q^2)$ because of the process $G \rightarrow Q\bar{Q}$ which feeds the $Q\bar{Q}$ sea — the B_N terms in (11). In practice it is convenient to express the q^2 dependence in terms of two free parameters; A and $R_0 = M_G(N, q_0^2)/M_2(N, q_0^2)$, the ratio of gluon to $(Q + \bar{Q})$ moments at q_0^2 , taken as 5 GeV^2 in the ABCLOS analysis. Fig. 9 shows the variation expected for $N = 4$, $\Lambda^2 = 0.5 \text{ GeV}^2$,

and for $R_0 = 0$ and 1, together with the data. Obviously, it is hard to determine the gluon moments without data of very high precision. Further, it is clear that one can trade off a change in Λ against a change in R_0 ; increasing Λ will make $M_2(N, q^2)$ change more

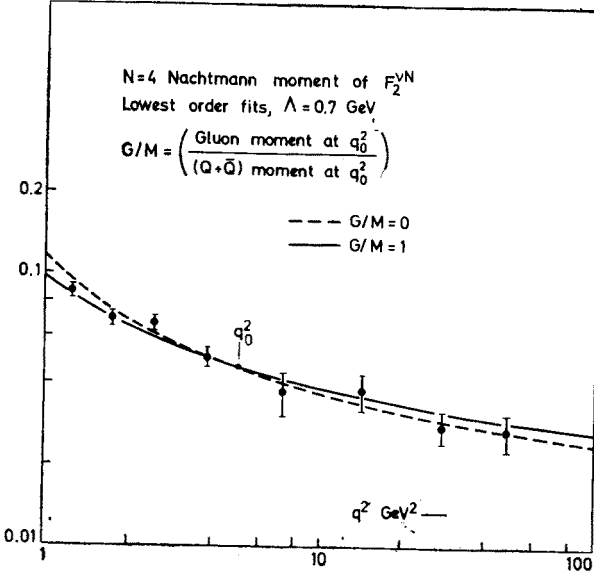


Fig. 9. Data points on F_2^{VN} moment versus q^2 (ABCLOS data). The curves show the variation expected for $\Lambda_{LO} = 0.50$ and for $R_0 = 1$ and 0, where $R_0 = (\text{gluon moment})/(F_2 \text{ moment})$ at $q_0^2 = 5$ GeV²

rapidly with q^2 , while increasing R_0 will damp down the q^2 dependence. The fits therefore give a relation between Λ and R_0 , as indicated in Fig. 10.

By feeding in the value of Λ from $M_3(N, q^2)$, the value of $M_G(N, q_0^2)$ can be read off (with a big error). The ABCLOS results [1] are given in Table III. In this table, we include also the results of Anderson et al. [3] from ep, ed, μp and μd data at SLAC and FNAL; they performed a simultaneous fit to the moments of u, d, s and c quarks and antiquarks, assuming some constraints e.g. $G(N, q_0^2) > 0$, $G(N, q_0^2) > G(N+1, q_0^2)$ etc. The CDHS group [6] have also recently reported results on gluon moments. Their data does not cover all values of q^2 at all x , so that they parametrize the parton distributions in the form $x^\alpha(1-x)^\beta$ where α, β are linear functions of $s = \ln(L_0/L)$, following the method of Buras and Gaemers [19]. They then compute moments and evaluate $M_G(N, q_0^2)$.

For $N = 2$, the gluon moment is known from momentum conservation; $M_G(2, q^2) = 1 - M_2(2, q^2)$; the corresponding values are given in brackets in Table III. Using this information, the ABCLOS group gave an independent estimate for $\Lambda = 0.68 \pm 0.06$ GeV from the F_2 analysis.

The main feature of Table III seems to be that, at $q_0^2 = 5$, gluon and $(Q + \bar{Q})$ moments are comparable. Of course, at larger q^2 , the gluon moments must fall off much more rapidly than the quark moments especially at high N , because of the $G \rightarrow G + G$ coupling of a non-Abelian field theory. A consistency check of the analysis can indeed be obtained

by evaluating $M_G(N, q_0^2)$ at different values of q_0^2 . One can then compare this with the predicted q^2 variation of M_G , as given by the second of the two singlet moment equations

$$M_{QS}(q^2) = M_{QS}(q_0^2) [(L_0/L)^{d^+} + A_N - R_0 B_N] ((L_0/L)^{d^-} - (L_0/L)^{d^+})] \quad (a),$$

$$M_G(q^2) = M_{QS}(q_0^2) [R_0(L_0/L)^{d^+} + (R_0 C_N - D_N) ((L_0/L)^{d^-} - (L_0/L)^{d^+})] \quad (b), \quad (12)$$

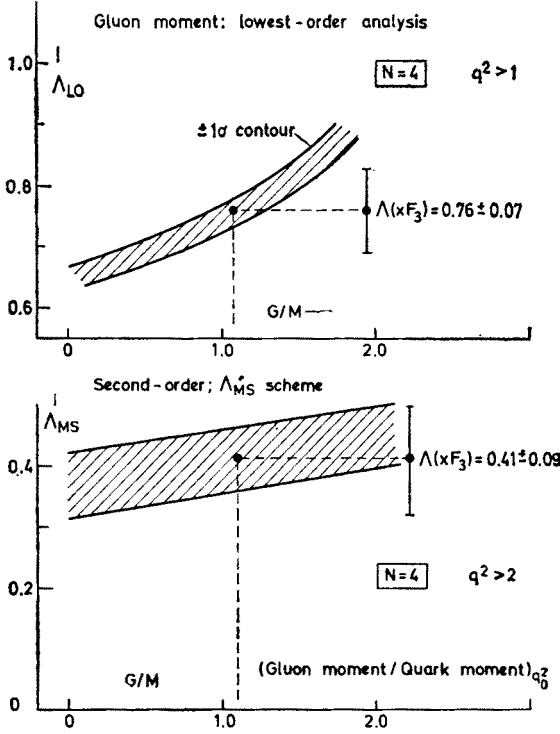


Fig. 10. 1 standard deviation contour indicating the correlation between Λ and R_0 , obtained by fitting the q^2 dependence of the $F_2^{\nu N}$ moment. Upper graph; leading order calculation. Lower graph; including next to leading order corrections

TABLE III

Gluon moments $G(N, q_0^2)$; $q_0^2 = 5 \text{ GeV}^2$

| N | ABCLOS [1] νN | | E98 [3] | CDHS [6] |
|-----|------------------------|-------------------|---------------|-----------------|
| | Valence Quark | | μN | νN |
| | $G(N, q_0^2)$ | $M_3(N, q_0^2)$ | $G(N, q_0^2)$ | $G(N, q_0^2)$ |
| 2 | 0.62 ± 0.15 (0.45) | 0.45 ± 0.07 | (0.43) | (0.51) |
| 3 | 0.12 ± 0.05 | 0.12 ± 0.02 | — | 0.11 ± 0.02 |
| 4 | 0.03 ± 0.02 | 0.045 ± 0.01 | 0.08 | — |
| 5 | 0.02 ± 0.02 | 0.027 ± 0.007 | — | — |
| 6 | — | 0.014 ± 0.003 | 0.02 | — |

where A_N, B_N, C_N, D_N are given in the Appendix. Anderson et al. [3] and de Groot et al. [6] confirm that the values of $M_G(N, q_0^2)$, obtained from (11) or (12a), for different q_0^2 , satisfy (12b).

In order to compare with the later gluon analysis in second order, a more illustrative way of presenting the results is to assume various values of R_0 and thence fit Λ from the F_2 moments. This procedure is shown in Fig. 11 for the ABCLOS data, where I have given

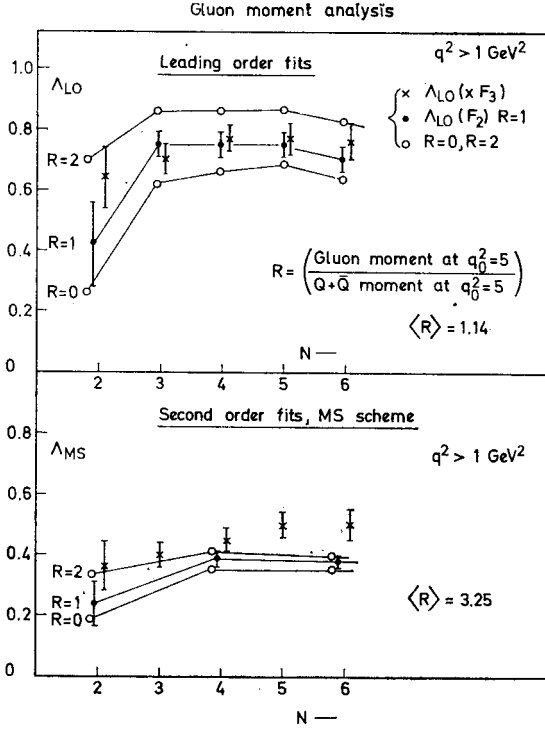


Fig. 11. Values of Λ as a function of N . Circles indicate the values obtained from fits to F_2 moments assuming $R_0 = 0, 1$ or 2 . Crosses indicate the fits to Λ from xF_3 moments. Upper graph; leading order calculation. Lower graph; including second order corrections

Λ for $R_0 = 0, 1$ and 2 (at $q_0^2 = 5 \text{ GeV}^2$) The Λ values from the non-singlet analysis are shown by crosses. It is satisfactory that the Λ values for $R_0 = 0$ and 2 straddle those from xF_3 , and that F_2 and xF_3 give roughly equal Λ values for $R_0 = 1$. Of course, if the same analysis were repeated for $q_0^2 = 50 \text{ GeV}^2$, say, the indicated R_0 values would be less, especially at large N^1 .

¹ $R_0 = 1$ is indicated for $N = 2$ from the momentum sum rule. However, for higher N , R_0 is a priori unknown. Values of $R_0 \sim 1$ or less seem likely however; it is difficult to believe that the gluon distribution would become harder than that of the quarks, at large N .

1.3. Higher Order Corrections

The strong coupling constant has the simple form (1) only for $\ln q^2/\Lambda^2 \gg 1$; in general higher order terms are involved:

$$\frac{\alpha_s}{\pi}(q^2) = \frac{A}{(\ln q^2/\Lambda^2)} + \frac{B}{(\ln q^2/\Lambda^2)^2} + \dots$$

For a value of $\Lambda^2 = 0.50 \text{ GeV}^2$, for example, $(\ln q^2/\Lambda^2)^{-1}$ varies from 1.44 at $q^2 = 1$ to 0.33 at $q^2 = 10$ and 0.19 at $q^2 = 100$. It is clear therefore that corrections of order $(\ln q^2/\Lambda^2)^{-1}$ are potentially important. Suppose we let $\Lambda \rightarrow \Lambda_1 = r\Lambda$, then

$$\frac{\alpha_s}{\pi}(q^2) \rightarrow \frac{A}{(\ln q^2/\Lambda_1^2)} + \frac{B - A \ln r^2}{(\ln q^2/\Lambda_1^2)^2} + \dots$$

Clearly, if the coefficient of the next to leading term is unknown, Λ is arbitrary; changes in Λ just amount to re-definition of this coefficient. The only thing we know for sure is that, in the LO fit, A and Λ_1 are chosen (by the data) so as to minimize the higher-order terms.

(i) *Non-Singlet Higher Order Effects.* Actual computations including the next to leading terms in the moment expressions have been carried out by Bardeen et al. [10] for the non-singlet. It is to be emphasized that, because third order terms are uncalculated, there is still some arbitrariness in Λ — to be dumped into the third order. Obviously, one only obtains the value of Λ from a calculation to all orders. The arbitrariness of choice of Λ — or equivalently, the coupling constant at fixed q^2 — corresponds to different choices for the renormalization scheme used. Bardeen et al. consider several schemes. One, labelled MS, uses the minimal subtraction scheme of t'Hooft, in which the non-singlet moment expression has the form

$$M_{\text{MS}}(N, q^2) = \frac{\text{const}}{(\ln q^2/\Lambda_{\text{MS}}^2)^{d_{\text{NS}}}} \left\{ 1 + \frac{B}{(\ln q^2/\Lambda_{\text{MS}}^2)} [A1 - A2(1 + \ln \ln q^2/\Lambda_{\text{MS}}^2)] \right\} \quad (13)$$

as compared with

$$M_{\text{LO}}(N, q^2) = \frac{\text{const}}{(\ln q^2/\Lambda_{\text{LO}}^2)^{d_{\text{NS}}}}.$$

In Eq. (13), $B = 3/(33-2m)$, $A1$ and $A2$ are functions of N given by Bardeen et al. In the region of N considered here, $A1$ and $A2$ are approximately proportional to N , with $A1 \sim 3A2$. Thus, for large N , the correction term can become very big, irrespective of q^2 . This stark fact is illustrated in Fig. 12.

Fig. 13 shows results of fits to Λ_{MS} and Λ_{LO} in the ABCLOS data. The quality of the fits. (i.e. the χ^2 for $q^2 > 1$) is much the same in the two cases; there has been no significant advantage in including the correction term. This is perhaps an unlucky accident of the numbers involved. In (13) the result of the two equations will be physically identical if we put

$$\Lambda_{\text{LO}} = r\Lambda_{\text{MS}},$$

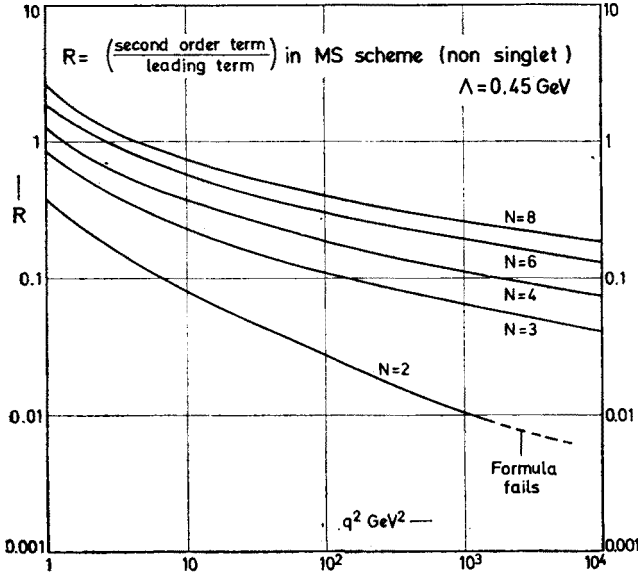


Fig. 12. Ratio of (next to leading order term)/(leading order term) in the MS renormalization scheme, using the formula of Bardeen et al. [10]. For $N = 2$, the correction term falls below 10% for $q^2 > 7$, while for $N = 4$, this occurs at $q^2 = 3000 \text{ GeV}^2$ and for $N = 8$, for $q^2 = 10^6 \text{ GeV}^2$

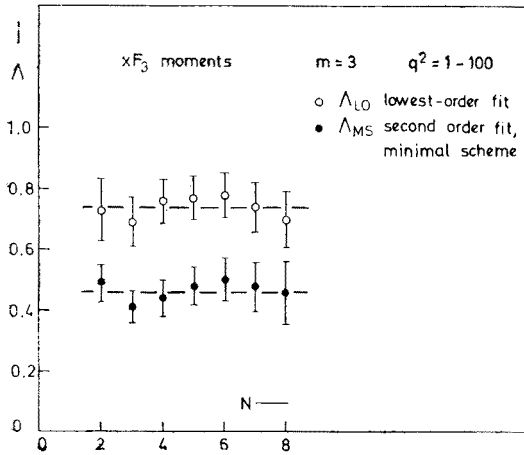


Fig. 13. Value of Λ_{LO} and Λ_{MS} versus N from ABCLOS data

where

$$\ln r = \frac{1}{2} BC(q^2) / (d_{NS} + (1 + d_{NS}) BC(q^2) / (\ln q^2 / \Lambda_{MS}^2))$$

with $C(q^2)$ equal to the content of the square bracket in (13). Fig. 14 shows the dependence of r on q^2 for 2 values of N . Roughly, r is a constant, of order 1.5–1.6, more or less inde-

pendent of q^2 or N . This explains how the χ^2 of the fits is the same, and that the fitted values

$$\langle A_{\text{MS}} \rangle = 0.45 \pm 0.05, \quad \langle A_{\text{LO}} \rangle = 0.75 \pm 0.05, \quad (14)$$

are related by a constant factor.

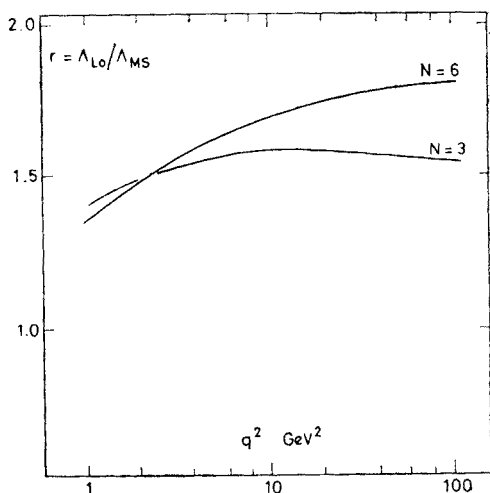


Fig. 14. The ratio $r = A_{\text{LO}}/A_{\text{MS}}$, as a function of N and q^2 , computed from the Bardeen et al. formulae. Since for $N = 3-7$ and $q^2 > 1$, r is roughly constant, the LO and MS schemes give equally good fits on non-singlet moments to the data and the fitted values of A_{LO} and A_{MS} are in a constant ratio

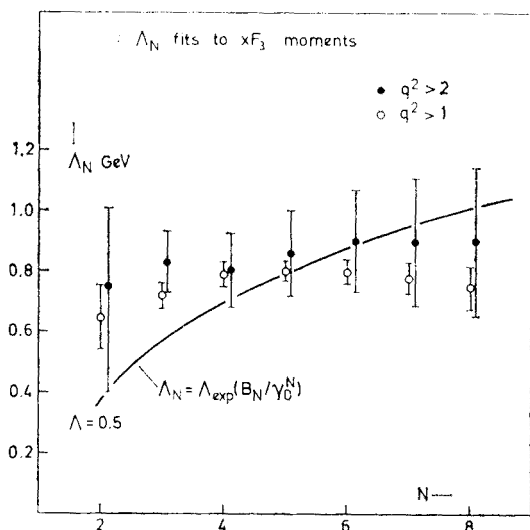


Fig. 15. Values of A_N versus N from data of Bosetti et al. The curve shows the variation $A_N = A \exp(B_0^N / \gamma_0^N)$ predicted by Bardeen et al. for $A = 0.50$

A second scheme, called the Λ_N scheme by Bardeen et al., seeks to absorb the expected N dependence of the next to leading order correction into the Λ value. Fig. 15 shows the resulting fits, together with the expected dependence

$$\Lambda_N = \Lambda \exp(B_N/\gamma_0^N), \quad (15)$$

where Λ is a constant, independent of N , and where B_N, γ_0^N are (complicated) functions of N given by Bardeen et al. (in practice, $\Lambda_N \sim 1.03 \Lambda_{LO}$). There is seen to be no experimental support for this scheme.

In view of the discussion in the first part of this section, one naturally expects *some* N dependence of the value of Λ obtained by fitting different moments, because the contributions from higher orders must in general be N dependent. The experiments so far are not good enough to detect such effects. All the data seem to be consistent with the notion that only the leading order term is important. Who knows, perhaps there are miraculous cancellations of the higher order effects!

(ii) *Higher Twist Effects, Resonance Contributions.* Everything so far has been under the assumption that only twist 2 operators (in the t -channel of the corresponding Compton

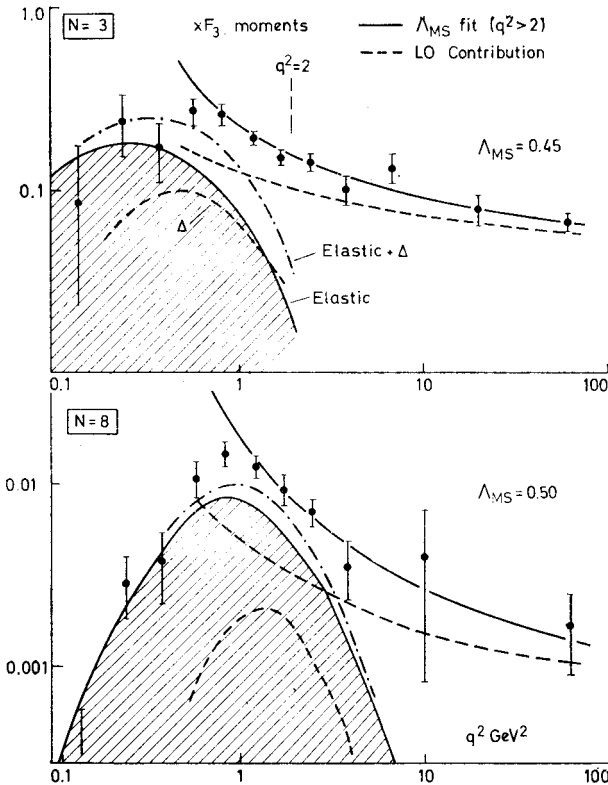


Fig. 16. The non-singlet moments $M_3(N, q^2)$ for $N = 3$ and $N = 8$ from the ABCLOS data. The curves indicate (i) the fits using the MS scheme, (ii) the calculated contributions to the moments from the elastic process $\nu N \rightarrow \mu N$ and from $\Delta(1238)$ production $\nu N \rightarrow \mu \Delta$

amplitude) enter the matrix elements for the inelastic cross-sections. Kinematic effects associated with twist 2 operators — the target mass term M^2/q^2 — have been taken care of by using the Nachtmann variable.

In the region $x \rightarrow 1$ (high N , low q^2) we expect effects from operators of twist 4 or more. These will contribute additional factors to the moments, of order m^2/q^2 , where m is a typical scale parameter, presumably of order Λ . The OPE approach does not tell us the precise form of these factors, but they could be of the form $(1 + N\Lambda^2/q^2)$, for example. It is fairly safe to say however that wherever the resonance region is important, twist 4 effects are potentially dangerous. We can avoid them only by going to small N and large q^2 . On the other hand, very precise experiments may, in the future, give us a handle on them.

This brings me to the sore point of the inclusion of elastic and quasi-elastic contributions in the ABCLOS and E98 analysis. Fig. 16 shows the elastic and Δ contributions to xF_3 , computed using standard dipole form-factors². For $N = 3$, elastic and Δ contributions are dominant at $q^2 = 1$, falling below 10% for $q^2 > 2$. However, for $N = 8$, elastic and Δ contributions extend to higher q^2 , falling below 10% only for $q^2 > 7$, i.e. they show the N/q^2 dependence surmised above. Clearly higher mass resonances of greater spin (threshold factors q^{2J}) will be prominent at still higher q^2 values. That is how the total cross-section is made up. One can see clearly from these graphs that the QCD fits fail for $q^2 < 1$ and that the first (elastic) resonance contribution falls off in that region. Presumably, because of duality arguments, any region of q^2 where *several* resonances contribute may be appropriate for testing QCD. Within the errors of the presently available data (10–15% on individual points) it is a fact that the fits are good for $q^2 > 1$ and for $N \leq 7$. As experiments improve, deviations due to high twist (or other) effects will doubtless be observed, but that has not happened yet.

(iii) *The Gross Llewellyn-Smith Sumrule.* For the case $N = 1$, the moment integral of xF_3 is called the Gross Llewellyn-Smith sumrule, and has the form

$$M_3(1, q^2) = 3 \left[1 - \frac{\alpha_s(q^2)}{\pi} + \dots \right]. \quad (16)$$

The appropriate Nachtmann moments are shown in Fig. 17 as a function of q^2 , [18]. These are lower limits, because the contributions to $\int xF_3 dx/x$ peak at small x and $x_{\min} = q^2/2ME(\max)$ where $E(\max)$ is the maximum beam energy. The curves show the form (16) for 3 values of Λ . The data appears to indicate $\Lambda < 0.5$ GeV.

One great advantage of using the $N = 1$ moment is that higher-twist contributions are expected to be very small.

(iv) *Higher-Order Corrections to the Singlet Moments.* Floratos et al. [11] have given formulae and tables for computation of singlet moments including next to leading order corrections, using the minimal subtraction (MS) scheme for renormalization. The results of this analysis of the ABCLOS data are given in Figs 10 and 11. These show that, in contrast

² I am indebted to Dr. Bianca Conforto (Firenze) for kindly supplying me with the program for the Λ (1238) structure functions, based on the Schreiner-Von Hippel parametrization of the Adler model.

to the leading order analysis, the gluon moments for $N = 4$ and $N = 6$ seem to become unphysical, i.e. require $R_0 \gg 1$. Furthermore, for these values of R_0 the χ^2 of the fits is unacceptably large. If we impose the condition $R_0 \leq 1$, we obtain values of $\Lambda_{\overline{MS}}$ from the F_2 and xF_3 moments which are significantly different. This again implies the importance

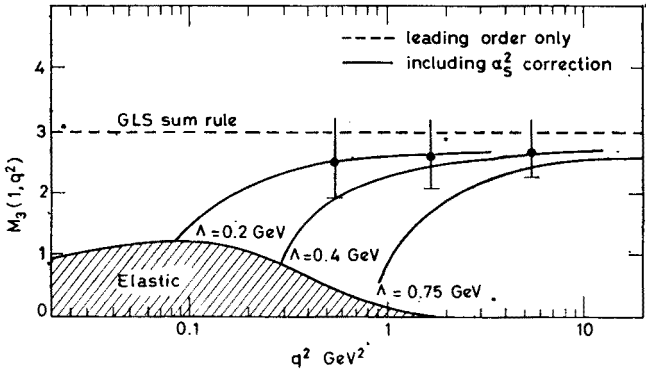


Fig. 17. CERN/GGM data on $\int_{0.02}^1 F_3 dx$ from Bosetti et al. The curves show the QCD corrections to the GLS sumrule, for 3 values of Λ

of other terms, with different effects on the singlet and non-singlet moments. The other feature of Figs 10 and 11 is that the sensitivity of the data to gluons — as measured by the spread in the fitted Λ for $R_0 = 0$ and 2 respectively — is about a factor 3 smaller than in the leading order fits. This also is a very strange result.

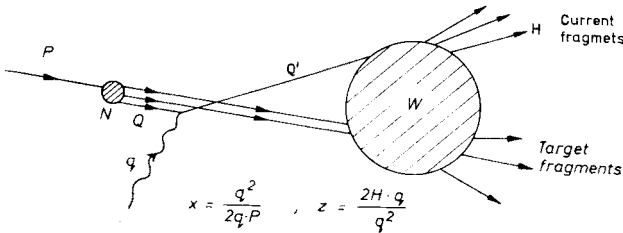
In short, the correction terms to the singlet moments, as computed in the \overline{MS} scheme, seem to give nonsensical results. This is very disappointing. In the non-singlet analysis, we saw that the correction terms did not improve the fits; for the singlet, on the contrary, they make everything worse.

PART II

Fragmentation Function Moments

2.1. Factorization, Fragmentation, Current and Target Fragments

The concept of the fragmentation of quarks into secondary hadrons is familiar from the work of Feynman and Field [14] and others. In the naive parton model, deep inelastic lepto-production of hadrons is viewed as a 2-stage process, and the cross-section has the form:



$$\frac{d^2\sigma}{dx dz} \propto x Q(x, q^2) D_Q^H(z, q^2), \quad (17)$$

where $Q(x, q^2)$ describes the distribution of quarks in a hadron, and the fragmentation function $D^H(z)$ the distribution of hadrons in the (struck) quark. The final hadrons have an invariant mass

$$W^2 = M^2 + q^2(1/x - 1)$$

and are divided into “current fragments” from the struck quark to which the above formula refers, and “target fragments” from the spectator quarks.

The important assumption in the above formula is that the cross-section *factorizes* into a product of a quark distribution, depending only on x and q^2 , and a hadron fragmentation function, depending on z and q^2 .

Whereas, in the process $e^+ e^- \rightarrow$ hadrons, the quantities q^2 and W^2 are identical, in lepto-production the two variables are independent. Typical (unpublished) results from

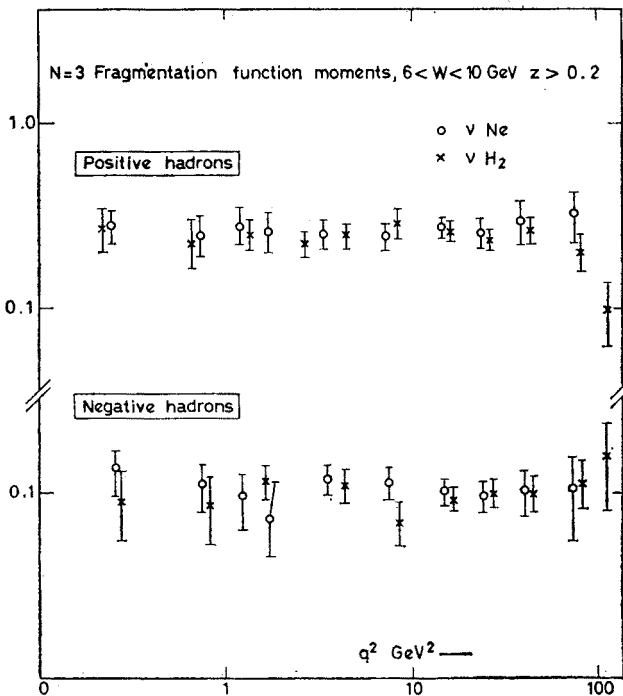


Fig. 18. $N = 3$ moments of fragmentation functions of positive and negative hadrons at fixed W , plotted against q^2 . Data from νH_2 experiment (ABCMO collaboration) and νNe experiment (ABCLOS) are shown separately

the ABCLOS and ABCMO neutrino experiments in BEBC, with Ne/H_2 and H_2 filling respectively, are given in Fig. 18, showing the $N = 3$ moment of the fragmentation function

$$M(q^2) = \int_{z_{\min}}^1 z^{N-1} D^{\pm}(z, q^2) dz, \quad (18)$$

where $D(z) = (1/N_{\text{event}})(dN_{\text{tracks}}/dz)$ is the multiplicity of secondaries, per event, per unit z interval. The data are plotted as a function of q^2 at fixed W . The limit $z_{\text{min}} = 0.2$ was imposed in order to select current fragments (see below).

It is clear from Fig. 18 that the moments M at fixed W depend very little on q^2 . Fig. 19 shows the $N = 2$ moments in the H_2 experiment as a function of x at fixed q^2 . At low values of $q^2 < 4 \text{ GeV}^2$, there is a substantial x dependence, M increasing with x , thus

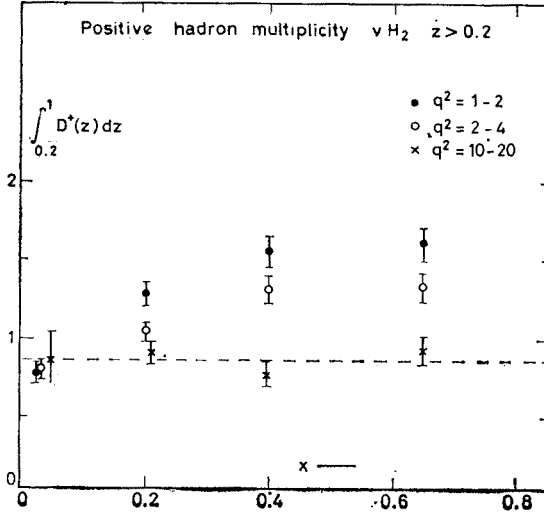


Fig. 19. $N = 1$ (= multiplicity) of positive hadrons as a function of x in 3 ranges of q^2 . Data from νH_2 experiment (B. Saitta, private communication)

reflecting an overall dependence on $W^2 \simeq q^2(1/x - 1)$. At higher $q^2(10-20)$, on the other hand, there is little x dependence. Thus the x dependence seems to be associated with the low W region; at high q^2 and W^2 , the data are consistent with the hypothesis of factorization. It is also clear, from consideration of contributions from the resonance region ($x \sim 1$, $z \sim 1$) that at small W and q^2 , factorization cannot apply.

If factorization does not apply generally, it has been suggested that one should really employ double moments [15]. The joint probability of observing a secondary H with a fraction z of the total hadron energy, from a quark carrying a fraction x of the target nucleon momentum, is denoted by a function $F^H(x, z, q^2)$ so that the double moment is

$$M(M, N, q^2) = \int_0^1 \int_0^1 x^N z^M F^H(x, z, q^2) dx dz / xz. \quad (19)$$

Writing the moment of the quark distribution

$$M_Q(N, q^2) = \int x^{N-1} Q(z, q^2) dx$$

the effective fragmentation moment is then defined by

$$M_F(M, q^2) = M(M, N, q^2) / M_Q(N, q^2), \quad (20)$$

where M_F should be independent of N . The point of all this is that, if $D(z, q^2)$ is x -dependent, it is not defined correctly by the track multiplicity $(1/N)(dN/dz)$ irrespective of event energy; at small x and low q^2 , events can be found at all incident energies, while at small x and high q^2 , they occur only at high energy. Thus $F^H(x, z, q^2)$ in (19) has to be determined by a proper integration over the incident neutrino spectrum. Today I am only reporting results of a preliminary analysis based on the simplifying assumption of factorization — the full double moment analysis has not yet been completed, but the differences are likely to be small³.

Finally, the definition of current fragmentation region needs some comment. Of course there is no unambiguous way to identify such hadrons; the approach is to try several reasonable assumptions and see how much the final results differ. One possibility is to define current fragments as those going forward in the CMS, i.e. require that x (Feynman) > 0 . The condition on $z = E(\text{hadron})/v$ is:



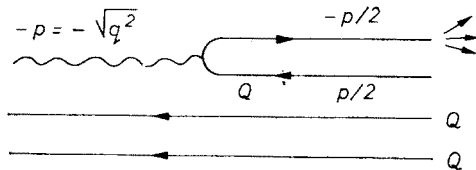
CMS

$$z > \frac{m}{\sqrt{q^2(1/x-1)+M^2}} \approx \frac{m}{\sqrt{q^2}} \sqrt{\frac{x}{1-x}} \quad \text{for } q^2 \gg M^2 x^2, \quad (21)$$

where m is the secondary hadron mass.

A second possibility is to choose particles travelling forward in the quark Breit frame, for which the condition is

$$z > \frac{m}{\sqrt{q^2}} \sqrt{1+4M^2 x^2/q^2} \approx \frac{m}{\sqrt{q^2}} \quad \text{for } q^2 \gg M^2 x^2. \quad (22)$$



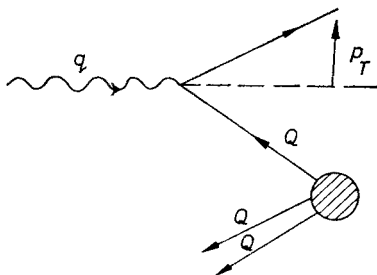
³ Since this report was prepared in December 1978, double moments have been calculated and first results presented by W. G. Scott at the Cal. Tech. Conference on QCD in February 1979. The results given here are effectively the double moments for $N = 1$ (i.e. weighted according to the quark momentum distribution), but are not corrected for the neutrino spectrum shape. For $N = 1$, the difference between the simple moment (18) and double moment (20) is however very small, since spectrum effects are important only at high q^2 , and as shown in Fig. 19, the cross-section then factorizes.

We should emphasize that the gluon fragmentation analysis is also based on the assumption of factorization, i.e. that the z distribution of gluon fragments does not depend on the x distribution of the gluons.

Since the Breit frame velocity in the lab. system is

$$\beta_{\text{BF}} = v/\sqrt{v^2 + q^2}$$

its use has no sense as $q^2 \rightarrow 0$, since then $\beta_{\text{BF}} \rightarrow 1$ — nothing can go forwards.



Eq. (22) is derived in the naive parton model. In fact, the quarks must possess primordial transverse momentum p_T , and in this case the above diagram is modified; hadrons travelling forwards with respect to the quark frame are not necessarily travelling forwards in the current frame. Formula (22) becomes modified to

$$z > \frac{m}{\sqrt{q^2}} \sqrt{\frac{1 + 4M^2 x^2 / q^2}{1 - (1 + 4M^2 x^2 / q^2) p_T^2 / q^2}}. \quad (23)$$

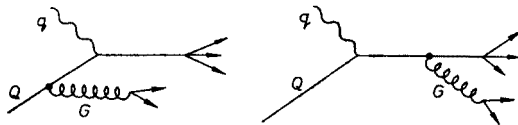
The quantity p_T should also include a contribution from the hadron relative to the fragmenting quark. To summarize; the bulk of the secondary hadrons are pions, and for these, one can either select those which are forward in the Breit-frame, or require the equivalent condition $q^2 > 1$ and $z > 0.2$; to avoid effects due to the intrinsic transverse momentum of the quarks, the condition $q^2 > 1$ is also required. These conditions do not guarantee that one will exclude target fragments, or include all current fragments. The uncertainties are largest for small N moments, which depend on the behaviour at small z . For larger values, they are unimportant.

The fragmentation moments quoted above do not include allowance for hadron mass effects; really one should use Nachtmann rather than Cornwall–Norton moments, i.e. replacing z by $\mathcal{Z} = 2z/(1 + \sqrt{1 + 4M_T^2 z^2 / q^2})$ where M_T is the transverse mass $\sqrt{M^2 + p_T^2}$ of a hadron. Since for pions, $M_T \sim 0.35$ GeV this correction is small for $q^2 > 1$ and has also been neglected in the preliminary analysis reported here.

2.2. Non-Singlet Fragmentation Moments

QCD makes predictions about the hadronic fragmentation of the quarks by virtue of the fact that the elementary quark and gluon constituents carry quantum numbers (charge, isospin, strangeness etc.) which will propagate through to the hadrons. In particular, we have seen that the relative contributions of the quark and gluon components

is q^2 -dependent. Since the fragmentation functions for quarks and gluons will in general be different, it follows that the overall fragmentation function will depend on q^2 .



Hard gluon bremsstrahlung contribution to fragmentation function

The derivation of the structure function moments in QCD was based on the operator product expansion (OPE). There is no equivalently rigorous treatment available for the fragmentation moments. However, on the simple argument that whatever formalism describes quarks in hadrons should equally describe hadrons in quarks, it is generally assumed that the logarithmic q^2 dependences and anomalous dimensions describing the structure functions will also apply to fragmentation [16, 17].

As in the case of structure functions, the most straightforward predictions about fragmentation are for the non-singlet moments. The fragmentation function combination

$$(D_{Q_i}^H - D_{Q_j}^H) \quad \cdot$$

where i and j are two different quarks, is clearly a flavour non-singlet. The singlet terms, corresponding to radiation by the quark of gluons (or $Q\bar{Q}$ pairs) cancel in taking the difference. For $Q_i = u$ and $Q_j = \bar{u}$, and applying charge conjugation, one finds $(D_u^{H+} - D_u^{H-})$ as a non-singlet. In neutrino interactions, one is dealing with quark transitions involving both valence and sea quarks. In the approximation $\theta_c = 0$ these are:

$$\nu + d \rightarrow \mu^- + u,$$

$$\nu + \bar{u} \rightarrow \mu^- + \bar{d}.$$

If we take account of the fact that the bulk of the secondaries are pions, then by isospin invariance

$$D_u^+ = D_d^- = D_d^+$$

and the difference of the fragmentation functions $(D^+ - D^-)_v$ is still a non-singlet. In any case, antiquarks make a very small ($< 10\%$) contribution in the q^2 range 1–100. Thus we expect that, in leading order in QCD,

$$M(N, q^2) = \int_0^1 z^{N-1} (D^+(z, q^2) - D^-(z, q^2)) dz = \frac{\text{const}}{(\ln q^2/\Lambda^2)^{d_{NS}}}. \quad (24)$$

In this equation, $\Lambda = \Lambda_{LO}$ is known from the moments of the structure function $x F_3$, so that the q^2 dependence of M is completely predicted, apart from one overall normalization constant.

Figs. 20 and 21 show some preliminary and unpublished results from the ABCLOS

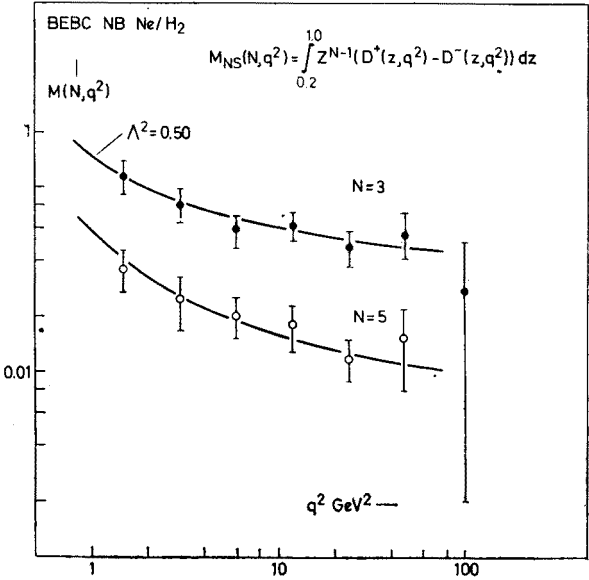


Fig. 20. Preliminary data on $N = 3$ and $N = 5$ moments of non-singlet fragmentation functions from Ne experiment. The curves indicate the QCD predictions for $\Lambda_{LO}^2 = 0.50$ (B. Saitta, private communication)

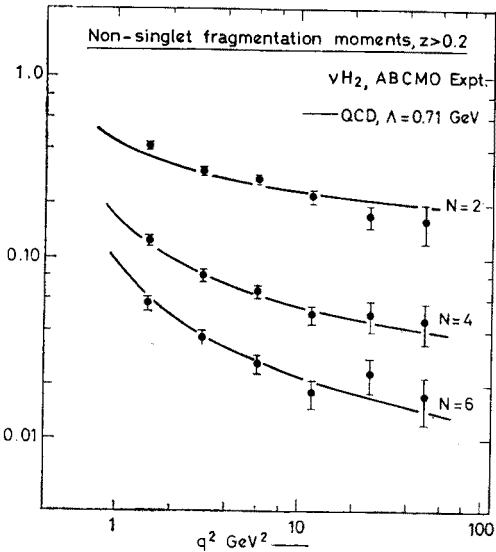


Fig. 21. As in Fig. 20, but data from νH_2 experiment (ABCMO collaboration)

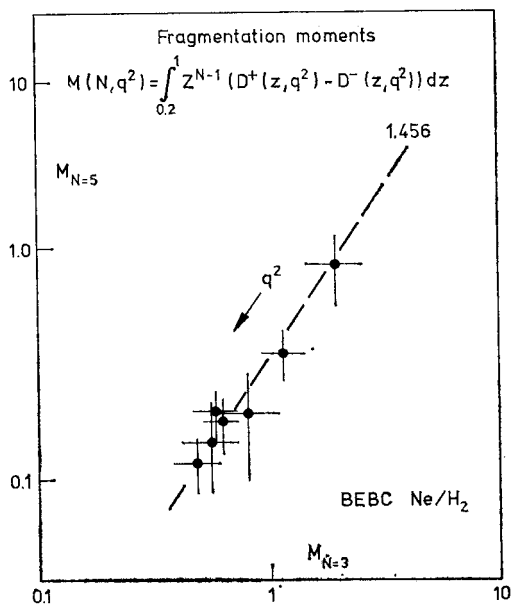


Fig. 22. Log-log moment plot of non-singlet fragmentation functions from ν Ne experiment

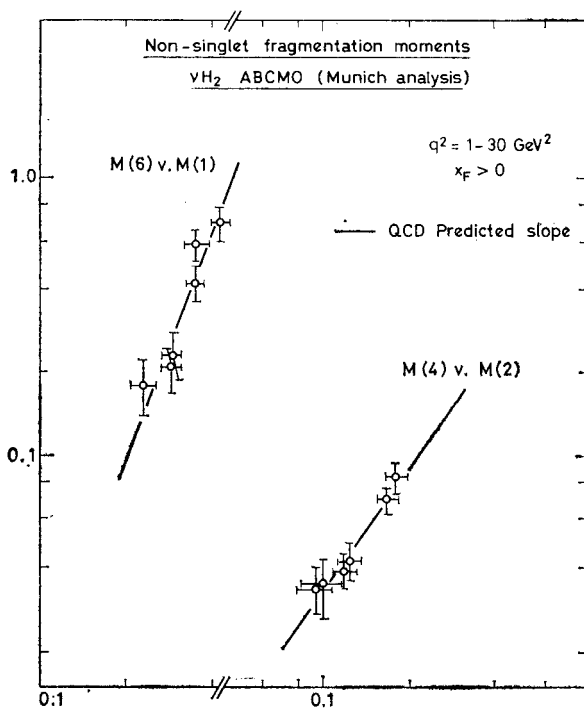


Fig. 23. As in Fig. 22, but from ν H₂ experiment. (N. Schmitz (Munich), private communication)

Ne/H₂ experiment, and from the ABCMO H₂ experiment⁴. The curves in each case show the prediction (24) for $A_{LO}^2 = 0.5$. In both cases, the agreement between theory and experiment, for $q^2 > 1$, is satisfactory. Figs. 22 and 23 show the corresponding results for the log-log plots of the non-singlet moments. The numbers in Fig. 23 are taken from an analysis of the ABCMO νH_2 data by the Munich group⁵. They used $x_{\mp} > 0$ to define the current fragments.

Finally, Fig. 24 shows the results for the fitted A_{LO} values, from the Munich analysis of the H₂ fragmentation data, and from the analysis of the non-singlet structure function $x F_3$ in the Ne/H₂ experiment described early on. I want to emphasize that the fragmenta-

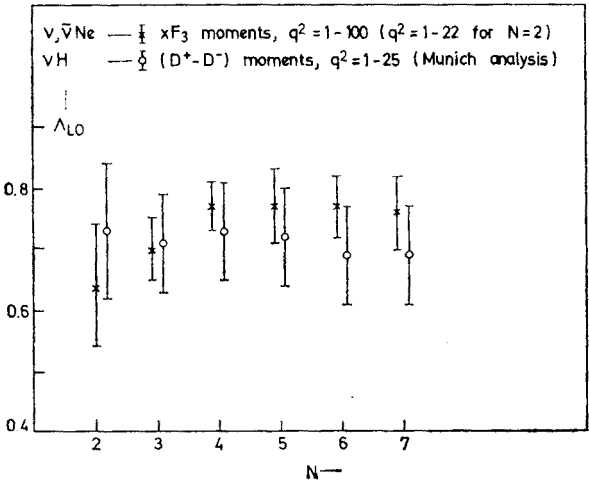


Fig. 24. Values of A_{LO} from analysis of non-singlet moments of xF_3 from $\nu, \bar{\nu} Ne$ data on structure functions (shown by crosses), and of $(D^+ - D^-)$ fragmentation functions in νH_2 data (shown by circles)

tion data are very preliminary and at this point ought not to be taken as definitive. The fact that, from two completely different methods of analysis of two independent experiments, the two estimates for A_{LO} agree within 5% is undoubtedly coincidence. However, that they should agree within 30% is already something of a miracle; when I plotted this graph I really began to believe — for the first time — that there might be something in QCD after all. Hopefully, the result will stand after further analysis and cleaning up of the data.

2.3. Gluon Fragmentation — The Singlet Moments

In exactly the same way that the moments of the F_2 structure function allowed us to extract something on gluon structure functions, we expect to get information on gluon fragmentation from the singlet combinations of hadrons. Following Uematsu [17] one

⁴ I am indebted to Dr. B. Saitta (Oxford) for kindly supplying this data.

can write the singlet quark fragmentation function as

$$D_{QS}^H = D_u^H + D_{\bar{u}}^H + D_d^H + D_{\bar{d}}^H + D_s^H + D_{\bar{s}}^H + \dots \quad (25)$$

and for the non-singlet

$$D_{QNS}^\pm = D_u^\pm - D_{\bar{u}}^\pm (= D_u^\pm - D_{\bar{u}}^\pm \text{ etc.}). \quad (26)$$

If we assume $m = 3$ quark flavours and SU3 symmetry, and the case where secondary pions are dominant, the “valence” (V) and “sea” (S) pion contributions can be written as

$$D_u^+ = V + S (= D_d^- = D_{\bar{u}}^- = D_{\bar{d}}^+), \quad (27)$$

$$D_u^- = S (= D_d^+ = D_{\bar{d}}^- = D_{\bar{u}}^+ = D_{s,s}^\pm). \quad (28)$$

Hence

$$\begin{aligned} D_{QS}^+ &= 2V + 6S, & D_{QNS}^+ &= V, \\ V + S &= (D_{QS} + 4D_{QNS})/6, & S &= (D_{QS} - 2D_{QNS})/6 \end{aligned} \quad (29)$$

and

$$\frac{D_u^-}{D_u^+} = \frac{S}{V + S} = \frac{(D_{QS}/D_{QNS}) - 2}{(D_{QS}/D_{QNS}) + 4}. \quad (30)$$

The last equation expresses the π^-/π^+ ratio in neutrino scattering in terms of the singlet/non-singlet functions, for which predictions are available from the leading order QCD formalism. The corresponding quark moments are:

$$M_{QNS}(N, q^2) = M_{QNS}(N, q_0^2) (L_0/L)^{d_{NS}}, \quad (31a)$$

$$\begin{aligned} M_{QS}(N, q^2) &= M_{QS}(N, q_0^2) [A_N(L_0/L)^{d_-} + (1 - A_N)(L_0/L)^{d_+}] \\ &\quad - M_{GS}(N, q_0^2) [H_N((L_0/L)^{d_-} - (L_0/L)^{d_+})] \end{aligned} \quad (31b)$$

and for the gluon moments

$$\begin{aligned} M_{GS}(N, q^2) &= M_{GS}(N, q_0^2) [A_N(L_0/L)^{d_+} + (1 - A_N)(L_0/L)^{d_-}] \\ &\quad - M_{QS}(N, q_0^2) [F_N((L_0/L)^{d_-} - (L_0/L)^{d_+})], \end{aligned} \quad (31c)$$

where the quantities A_N , F_N and H_N , depending on N and m , as well as the anomalous dimensions d_{NS} , d_+ , d_- are given in the Appendix. M_{GS} is the gluon fragmentation moment, and $L_0 = \ln q_0^2/\Lambda^2$, $L = \ln q^2/\Lambda^2$, where q_0^2 is the reference value of q^2 . Given the value of Λ , (30) and (31) together can be used to express the ratio of π^- to π^+ moments in neutrino scattering at any q^2 in terms of the measured ratio at q_0^2 , and the ratio of gluon to quark singlet moments at that point. The point of choosing the π^-/π^+ ratio — rather than the sum ($\pi^+ + \pi^-$) — is that it is particularly sensitive to the gluon moments, and not strongly dependent on Λ .

Preliminary results for M^-/M^+ and for $N = 2$ and $N = 6$, are shown in Fig. 25. The curves are given for different assumed values of

$$P_0 = 6M_{GS}^\pm(N, q_0^2)/M_{QS}^\pm(N, q_0^2). \quad (32)$$

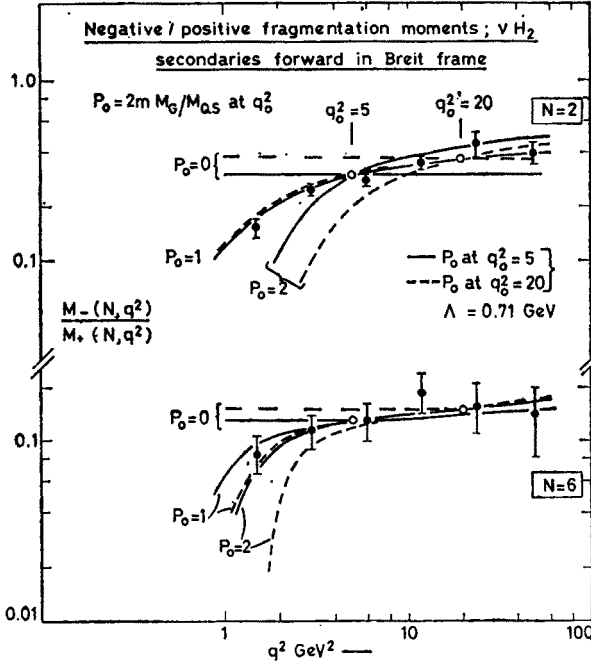


Fig. 25. Preliminary BEBC data on ratio of moments of negative and positive hadron fragmentation functions, from νH_2 experiment, versus q^2 , for $N = 2$ and $N = 6$. The curves are QCD predictions, for different values of P_0 = (gluon fragmentation moment)/(singlet quark fragmentation moment) at q_0^2 . Solid curves, $q_0^2 = 5 \text{ GeV}^2$; broken curves, $q_0^2 = 20 \text{ GeV}^2$

For the $N = 2$ moment, energy-momentum conservation implies that, if we sum over all secondaries, neutral and charged, then

$$\begin{aligned} \sum^H M_{QS} &= \sum_{i=1}^H \sum_{j=1}^{2m} \int_0^1 z D_{Q_i}^H(z) dz = 2m (= 6), \\ \sum^H M_{GS} &= \sum_{i=1}^H \int_0^1 z D_G^H(z) dz = 1. \end{aligned} \quad (33)$$

In the νH_2 experiment, only charged secondaries are measured, as implied in (32). Nevertheless, we might expect $P_0 \simeq 1$, the same as the value if we included neutrals. The $N = 2$ results are indeed consistent with $P_0 \simeq 1$. What is very satisfactory is that this is true for both $q_0^2 = 5 \text{ GeV}^2$ and $q_0^2 = 20 \text{ GeV}^2$ — as indeed it should be, since (33) is valid at all q^2 .

The data for $N = 6$ show, on the contrary, different values of P_0 depending on the choice of q_0^2 . For $q_0^2 = 5$, $P_0 \simeq 2$, while for $q_0^2 = 20$, $P_0 \simeq 1$. Thus, relative to the (singlet)

quark moment M_{QS} , the $N = 6$ gluon moment M_{GS} falls off more rapidly with q^2 . This is precisely what is found from Eq. (31c), predicting a factor 1.8, and arises, as pointed out in the discussion on structure functions, from the $G \rightarrow G + G$ diagram.

When the quark and gluon fragmentation moments have been fully evaluated, an obvious application would be to predictions for the process $e^+e^- \rightarrow$ hadrons, on and off resonance. Off resonance, the "2 quark jet" annihilation

$$e^+e^- \rightarrow \sum_i (Q_i + \bar{Q}_i) \rightarrow \text{hadrons} \quad (34)$$

is described by D_{QS} (weighted however by the quark charges, squared). At prominent resonances ψ , Υ ... the dominant process is proposed to be

$$e^+e^- \rightarrow \Upsilon \rightarrow 3G \rightarrow \text{hadrons} \quad (35)$$

and is described by D_{GS} .

As q^2 increases, D_{GS} peaks to low z more rapidly than does the function D_{QS} for the quarks. Hence, high mass 1^- resonances ($b\bar{b}$, $t\bar{t}$...) decaying via the 3-gluon channel, should exhibit higher multiplicities and softer z distributions than the off-resonance quark-antiquark jets.

Let me emphasize that I have discussed partial and preliminary data from the Aachen-Bonn-CERN-Munich-Oxford BEBC wideband νH_2 experiment. They serve mainly to illustrate the sort of physics that one can get out. In the future, better statistics, including, hopefully, information on d-quark decays from antineutrino runs, will be forthcoming.

2.4. Quark Charges

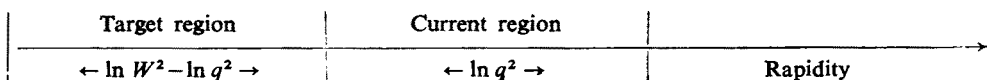
As a final application of ideas on fragmentation one can consider the $N = 1$ moments of the non-singlet fragmentation function, which should measure the quark charges, i.e.

$$\begin{aligned} \int_0^1 (D_u^+ - D_u^-) dz &= \frac{2}{3} - \delta, \\ \int_0^1 (D_d^+ - D_d^-) dz &= -\frac{1}{3} - \delta, \end{aligned} \quad (36)$$

where $\delta \sim 0.06$ is a small correction applied by Feynman and Field [14] to take account of SU3 symmetry breaking (i.e. $s\bar{s}/u\bar{u} < 1$ for the quark-antiquark sea). We can, in principle, measure the quantities in (36) using neutrino and antineutrino reactions

$$\nu + d \rightarrow \mu^- + u, \quad \bar{\nu} + u \rightarrow \mu^+ + d$$

if we keep to the region $x > 0.1$ so as to exclude, as far as possible, the diluting effects of the sea quarks. Actually there are competing demands with respect to the appropriate x region to use. In order to separate the wanted current fragments from the unwanted target fragments, we need to keep the rapidity interval between the two as large as possible



Thus we need $(\ln W^2 - \ln q^2)$ large i.e. x fairly small, while the need to separate valence from sea quarks requires x not too small. The choice $x > 0.1$, $W > 4$ GeV is a compromise — not necessarily the best. Because of the confusion between target and current fragments one cannot expect very reliable estimates of the charge. The situation is different from that for the higher N moments, where the target region is killed off by the z^{N-1} factor.

Fig. 26 shows the results obtained by Scott [18] using the BEBC Ne/H₂¹ data from neutrinos and antineutrinos. The charge per event per interval of $\ln z$ is plotted

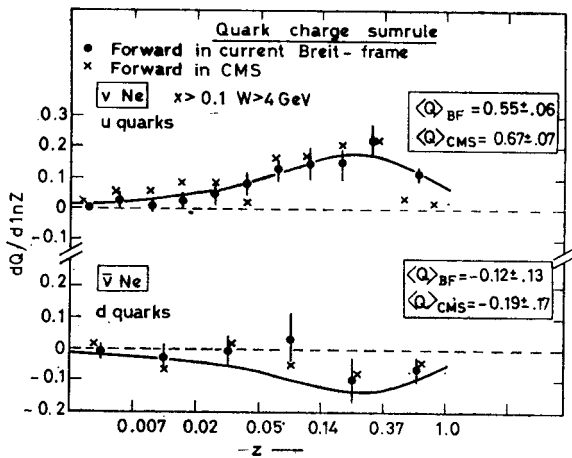


Fig. 26. Contribution to the $N = 1$ non-singlet moments of the fragmentation functions as a function of z , for ν Ne (top) and $\bar{\nu}$ Ne (bottom) reactions. The integral of the distributions should measure the quark charges $\langle Q_u \rangle$ in the upper graph and $\langle Q_d \rangle$ in the lower. The curves are from the Feynman-Field prediction [14]. The current fragments are defined as hadrons forward in the CMS (crosses) or forward in the quark Breit-frame (circles) (After W. G. Scott [18])

against z , measured either in the Breit frame or centre-of-mass frame ($z_{\text{BF}} = 2p_L^{\text{BF}}/\sqrt{q^2}$, $z_{\text{CMS}} = 2p_L^{\text{CMS}}/W$ and both are close to the lab. system value $z = E^H/\nu$). The plot in terms of $\ln z$ was chosen to facilitate comparison with Feynman and Field. The results of the integration (35) are given in the table below:

TABLE IV

| Quark charges [18] $\nu, \bar{\nu}$ Ne (ABCLOS) | | |
|---|-----------------------|-----------------------|
| | $\langle Q_u \rangle$ | $\langle Q_d \rangle$ |
| Breit-frame | $+0.55 \pm 0.06$ | -0.12 ± 0.13 |
| CMS | $+0.67 \pm 0.07$ | -0.19 ± 0.17 |
| Feynman-Field | $+0.60$ | -0.39 |

The large errors on Q_d are directly due to the very small number (~ 270) of antineutrino events available. This shortcoming will be made good with more data which have been taken in the last month or so.

Clearly, these results do not prove that the quarks have the fractional charges $+2/3$ and $-1/3$ that we know and love so well, but they are consistent with such assignments.

Summary and Conclusions

The most important experimental result on this subject over the last year is that *all* experiments on lepton-nucleon scattering now see significant deviations from Bjorken scaling, whether one uses the Bjorken x or the Nachtmann variable ξ .

Most of the experiments see rather gentle dependence of the structure functions on q^2 , qualitatively similar to the logarithmic dependence expected from the asymptotically free gauge theory of quarks and gluons (QCD). There is one experiment on muon-Fe scattering at FNAL, by Chen, which I did not mention, which reports very much stronger q^2 dependence at high q^2 ($q^2 > 50$). No other experiments see this, but they have limited data in this region. Even the gentler q^2 dependences may be due to other things (thresholds, new phenomena) than QCD effects — but since my brief was comparison with QCD, that is what I concentrated on.

For the structure functions, there is data from one muon scattering experiment (E98) in H_2 and D_2 , and from two neutrino experiments (CDHS and BEBC ABCLOS) using isoscalar targets. They all find non-singlet moments of different orders which are related by power laws with indices more or less consistent with QCD (vector gluons). Furthermore, the $N = 1$ moment sumrule (GLS) is in good shape. The scale parameter Λ (measured in QCD leading order) is ~ 0.7 GeV in 2 experiments and much smaller (~ 0.4 GeV) in a third. So, more work needs to be done! The analyses of the gluon moments also lead to sensible results, with the lower moments comparable with those of the quarks.

Calculations have also been made, for both singlets and non-singlets, with inclusion of terms in next to leading order. The results are disappointing; none of the fits are better than those in leading order, and some are much worse.

A considerable amount of progress is being made right now in the analysis of fragmentation functions. The non-singlet moments seem to come out with the same anomalous dimensions and Λ values as was found for the structure functions, and this result, if confirmed, will be a real triumph for the theory. The $N = 1$ moments are consistent with the fractional quark charge assignments. The singlet moment analysis leads to estimates for gluon fragmentation moments, from which the actual fragmentation functions can, eventually, be derived. An important cross-check of these findings will be to processes like $e^+e^- \rightarrow \gamma \rightarrow 3G \rightarrow \text{hadrons}$.

My feeling is that most of the easy experimental measurements, and the qualitative or semi-quantitative comparison with QCD, have now been done. It will be clearly a very much harder task to reduce the experimental errors by even a modest (~ 3) factor and to match this improved precision by more detailed theoretical calculations, involving higher-order corrections. Neutrino experiments, if done with bubble chambers, are of very limited

statistical precision and can hardly contribute very much more on this subject; counter experiments have enormously better statistical precision but the present generation of calorimeters, plus solid magnetized iron toroids for muon momentum analysis, are strongly limited by their relatively poor resolution and by other sources of systematic error. Perhaps the best hope lies in high statistics, high precision muon scattering experiments, and I hope for great things from the CERN EMC experimental programme. But it all looks like being quite hard and personally I feel this may be a good time to get out and do other things.

APPENDIX

The parameters A_N , B_N , C_N , D_N , F_N , H_N , d_{NS} , d_+ and d_- quoted in equations (11) and (31) have the following values (using the Hinchliffe-Llewellyn-Smith notation [13]):

$$d_{\pm} = \frac{1}{2} [d_{NS} + d_{GG} \pm \sqrt{(d_{NS} - d_{GG})^2 + 4d_{QG}d_{GQ}}],$$

$$d_{GG} = \frac{9}{(33-2m)} \left[\frac{2m}{9} + \frac{1}{3} - \frac{4}{N(N-1)} - \frac{4}{(N+1)(N+2)} + 4 \sum_2^N \frac{1}{j} \right],$$

$$d_{GQ} = \frac{-8(N^2 + N + 2)}{(33-2m)N(N^2-1)}, \quad d_{QG} = \frac{-6m(N^2 + N + 2)}{(33-2m)N(N+1)(N+2)},$$

$$d_{NS} = \frac{4}{(33-2m)} \left[1 - \frac{2}{N(N+1)} + 4 \sum_2^N \frac{1}{j} \right], \quad A_N = (d_+ - d_{NS})(d_+ - d_-),$$

$$B_N = d_{QG}/(d_+ - d_-), \quad C_N = (d^+ - d^{GG})/(d_+ - d_-) = (1 - A_N),$$

$$D_N = d_{GQ}/(d_+ - d_-), \quad F_N = A_N C_N / (2m D_N), \quad H_N = 2m D_N.$$

REFERENCES

- [1] P. Bosetti et al., *Nucl. Phys.* **B142**, 1 (1978).
- [2] H. L. Anderson et al., *Phys. Rev. Lett.* **38** (1977); **36**, 1422 (1976).
- [3] H. L. Anderson et al., *Phys. Rev. Lett.* **40**, 1061 (1978).
- [4] T. Quirk, Proc. Copenhagen Symposium *Jets in High Energy Collisions*, 10-14-th July, 1978 (to appear in *Physica Scripta*).
- [5] E. M. Riordan et al., SLAC-PUB-1634; W. E. Atwood, SLAC-PUB-185 (1975).
- [6] J. de Groot et al., *Comparison of Moments of Valence Structure Function with QCD; Inclusive Interactions of High Energy Neutrino and Antineutrinos in Iron*, CERN preprints, Nov. 1978; *QCD Analysis of Charged Current Structure Functions*, Dortmund preprint, Dec. 1978.
- [7] G. Altarelli, G. Parisi, *Nucl. Phys.* **B126**, 298 (1977).
- [8] O. Nachtmann, *Nucl. Phys.* **B63**, 237 (1973); **B78**, 455 (1974).
- [9] S. Wandzura, *Nucl. Phys.* **B112**, 412 (1977).
- [10] W. A. Bardeen et al., FNAL-PUB-78/42THY (1978).

- [11] E. G. Floratos, D. A. Ross, C. T. Sachrajda, CERN Thy 2570 (1978).
- [12] E. G. Floratos et al., *Nucl. Phys.* **B129**, 66 (1977); A. J. Buras et al., *Nucl. Phys.* **B131**, 308 (1977).
- [13] I. Hinchliffe, C. H. Llewellyn-Smith, *Nucl. Phys.* **B128**, 93 (1977).
- [14] R. P. Feynman, R. D. Field, *Nucl. Phys.* **B136**, 1 (1978).
- [15] J. Ellis, M. K. Gaillard, W. J. Zakrzewski, CERN Thy 2595 (1978).
- [16] R. K. Ellis et al., *Phys. Lett.* **78B**, 281 (1978).
- [17] T. Uematsu, *Phys. Lett.* **79B**, 97 (1978).
- [18] W. G. Scott, Proc. Copenhagen Symposium *Jets in High Energy Collisions*, 10–14th July 1978 (to appear in *Physica Scripta*).
- [19] A. J. Buras, K. J. Gaemers, *Nucl. Phys.* **B132**, 249 (1978).